Origin of Late Noachian-Early Hesperian Valley Networks on Mars: Insights from an Integrated Multi-Analysis Technique Approach.

K. R. Karpenko[1], J. L. Fastook[2], J. W. Head[3], A. D. Howard[4], C. I. Fassett[5], J. L. Dickson[6], K. E. Scanlon[3], B. D. Boatwright[7]. *[1]Los Altos High School, Los Altos CA, USA, [2]University of Maine, Orono ME, USA, [3]Brown University, Providence RI USA, [4]University of Virginia, Charlottesville VA USA, [5]John Hopkins University Applied Physics Laboratory, Laurel MD, USA, [6]University of Minnesota, Twin Cities MN USA, [7]Mt. Holyoke College, South Hadley MA USA.*

Introduction: One of the most controversial aspects of the history of Mars is the origin of the distinctive and widespread valley network (VN) systems [1], and the implication of their presence for the nature of the ambient climate during their formation. Dated to a concentration around the Late-Noachian/Early Hesperian [2], all would agree that the surface flow of liquid water (fluvial activity) was involved in their formation, but the origin of the flowing water, whether it was continuous, intermittent or episodic, and its relation to the ambient atmosphere is highly debated. Two end-member hypotheses have emerged:

1) A 'Warm and wet/warm and arid" scenario, where MAT is =/> 273 K, and atmospheric precipitation, primarily rainfall (pluvial), and subsequent water infiltration and runoff, formed the VN [3-5]. Typically, this scenario also includes a robust and *vertically integrated hydrological system* and cycle, where rainfall infiltrates into the groundwater system, connected to bodies of water in the northern lowlands. Runoff in the VN, interrupted by open- and closed-basin lakes, adds surface water to the Northern Lowland bodies of water. Evaporation from these Northern Lowland bodies of water feed the precipitation in the VN headwaters, completing the hydrological cycle.

2) A 'Cold and icy highlands' scenario, in which MAT is ~225 K, and atmospheric pressure is sufficient to induce an adiabatic cooling effect. In this scenario, any water in the 'warmer' Northern Lowlands ablates and is precipitated out as snowfall (nivial) in the southern uplands and south polar region, forming glacial-like accumulations of ice [6-9]. The observed fluvial activity is interpreted to be derived from episodic melting of the upland ice deposits, and drainage downslope to form the fluvial channels and open-closed basin lakes. The hydrological system is not vertically integrated, but rather *horizontally stratified*, with a global ice-cemented cryosphere separating the surface from any deeper groundwater system.

In our work, we adopt a multidisciplinary, integrated, multi-analysis technique approach, utilizing the morphological and morphometric aspects of the VN systems and their environments, to attempt to distinguish between these two end-member hypotheses and to outline critical new observations and analyses that will further elucidate the nature of the Late Noachian-Early Hesperian ambient climate and associated processes.

Methods and Methodology:

1.1 Data. The ground truth digital elevation model (DEM) was sourced from the MOLA/HRSC dataset. The study site was chosen for exhibiting well-preserved, dendritic valley networks; Warrego Valles met these criteria and was therefore selected as the primary study area. The global mosaic was clipped to Warrego Valles, and then resampled to a cell size of ~0.5 km. To create the initial conditions surface (ICS), the VN mapped by [10] and superimposed craters from [11] were buffered and the 'Extract by Mask' tool in ArcGIS Pro was used to remove these areas from the DEM surface. The 'Natural Neighbor' interpolation tool was then utilized to infill the extant valleys, finalizing the pre-incision surface. The ICS, and all ensuing rasters and shapefiles, were projected using a custom projection centered on Warrego Valles in order to minimize the effects of distortion. Qualitative evaluation was performed based on Hillshade views of model output surfaces (MOS) DEMs, as well as orthoimages derived from the Context Camera (CTX) aboard the Mars Reconnaissance Orbiter, and served to validate the quantitative results.

1.2 Landform Evolution Modeling. MARSSIM is a robust program for Mars landform evolution modeling and has been used for several sophisticated studies on fluvial incision and the Noachian paleoclimate [12-15]. MARSSIM does not include support for a Cold-Icy melting mechanism, and therefore a meta-program was created to exert greater control over the spatial-temporal nature of modeled discharge release. Mars' axial tilt oscillates between ~15° and 45°, with a ~120 ka periodicity, as shown by numerical integrations of Mars' orbital dynamics [16]. During high-obliquity excursions, increased polar summer insolation mobilizes water vapor into the atmosphere and deposits snow and ice at mid-latitudes [17]. The ice sheet terminus was parametrized to periodically oscillate between a minimum and maximum altitude at a cycle length of 120 ka. Meltwater was only released during the retreat phase, and did not occur when the ice sheet advanced. 150, 200, and 250 emitter points were uniformly emplaced on the altitude line, and emitted discharge equally. A random jitter of several cells was introduced to ensure that valley heads were allowed to form at varying positions in each successive retreat cycle. For precipitation-based runs, we explore uniform, and elevation-dependent variants. A hierarchical, multi-level parameter study was performed in MARSSIM for each end-member variant. The first stage entailed a systematic exploration of the internal MARSSIM parameters. For variants

incorporating a meta-program, the investigation progressed to a second stage in which higher-level driver parameters were analyzed.

1.3 Climate Modeling. 3-D Global Climate Models (GCM) have been unable to match the distribution of rainfall in a Warm-Wet scenario to VN [7-8, 18]. Therefore, we cannot utilize Warm-Wet derived GCM outputs to gain new insights through landform evolution modeling. However, Cold-Icy GCM have reproduced the spatial layout of Mars's valleys and have been integral to the construction of the Late Noachian Icy Highlands (LNIH) hypothesis [8-9, 18-20]. We use data from a 1 bar CO_2, 42° obliquity run of the LMD Mars GCM [21] for ice sheet mass-balance modeling.

1.4 Ice Sheet Modeling. The University of Maine Ice Sheet Model (UMISM) has been successfully applied to the mass-balance modeling of paleo ice sheets on Mars [9]. LMDZ climate fields for a high obliquity scenario were applied to define local ice-sheet extent. The resulting margins were used to validate the lower bound of the elevation band over which the terminus advanced and retreated. The model was run with an inset over Warrego Valles and predicted a ~4 km high-obliquity ELA.

1.5 Quantitative Analysis. For each output DEM we subtract the initial surface to get a raster of positive incision depths. The run is terminated when the 95-percentile depth reaches the target value, which ensures that all simulations end at comparable morphologic stages. Given the heavily modified state of many VN, we apply a survivability bias and restrict our analysis to only a select number of sub-catchments. A morphological-based delineation method was applied to reduce false positives and ensure more accurate metric computation [22]. An ArcGIS Model Builder routine was created to generate the confluences, snapped pour points (outlets are relocated to the highest flow accumulation value within a 6 km radius; used for defining the watersheds), main trunk, and watersheds, which served as necessary inputs for metric computation. A Python script then computed highest stream order, drainage density, Hack's exponent, bifurcation ratio, as well as branching angle and headwater elevation histograms [23-28]. The fixed-terminus scenario is predicted to yield lower stream orders, reduced drainage density, and smaller bifurcation ratios than the precipitation variant [28]. It is also expected to produce a tightly clustered headwater-elevation distribution, whereas the precipitation case should exhibit a broader, more uniform spread [27]. Anticipated differences in Hack's exponent and branching angle are less definitive and will be examined in the analysis that follows. While these metrics have all been used to infer climate conditions behind the formation of the observed fluvial features, this study also serves to discern whether each metric can morphologically distinguish between the Warm-Wet and Cold-Icy ADELAM (Advanced Discharge ELA Model; representing the retreating and advancing ice sheet parametrization) endmembers. Principal component analysis (PCA) was then employed [28], and the z-scored Euclidian distance was computed between each run feature and the ground truth.

Results:

1. Metrics. Warm-Wet Uniform and Cold-Icy ADELAM runs repeatedly matched ground truth values for drainage density (0.22-0.30 km^{-1}), branching angles (40-55°), and headwater elevations (EMD 300-800 m), while producing the full hierarchical depth (max Strahler order 5-6). In contrast, fixed terminus VN showed sparse dissection (0.09 km^{-1}), narrower angles (< 38°), and a large headwater mismatch (1200 m). When comparing headwater elevation histograms, fixed terminus runs exhibited a peak at the injection line, which aligns with the results of [27], however ADELAM runs exhibited a broader, flatter distribution, comparable to that of the precipitation runs as well as the ground truth. Hack's exponent showed minimal spread across all endmember variants. Neither the bifurcation ratio nor the network-wide mean branching angle matched the ground truth; and as branching angle is not typically measured for all tributaries [26], we retained only the mean branching angle of tributaries merging into the main trunk.

2. Cumulative Analysis. In PCA, the first two components captured ~80% of the variance, and the first and third components captured ~74% of the variance. These two plots also confirmed the pattern that was observed through the individual metrics: Warm-Wet Uniform and Cold-Icy ADELAM runs formed a cluster near the ground truth, while the Cold-Icy Fixed runs formed an isolated cluster along negative PC1.

Discussion and Conclusions: We now address the metric predictions given for each endmember variant scenario as well as the questions we have put forth, utilizing the data derived from this robust pipeline.

1. *Can Cold-Icy runs achieve morphology comparable to that of the ground truth?*

Fixed terminus runs are unable to match the morphometry exhibited by the ground truth and aligns with the predicted lower drainage densities and the distribution of headwater elevations. Dissection rates are low, and limited valleys form at lower elevations. In stark contrast, the ADELAM runs display high drainage density, stream orders, and bifurcation ratios, as well as the broad distribution in headwater elevations interpreted as a clear sign of pluvial activity [27]. Through the individual and cumulative analysis, we can observe that ADELAM runs produce comparable morphology and morphometry to Warm-Wet runs and the ground truth.

2. *What metrics can be used to capture meaningful differences between modeled VN?*

Among the six quantitative metrics assessed, five displayed distinct variability and clustering, whereas Hack's exponent did not. Because Hack's exponent is thought to capture an inherent fractal property, its insensitivity to the different model scenarios is expected [29-30]. Although branching angle is largely dictated by local topography, which potentially limits its value in interregional comparisons, it remains appropriate in this study, where topography is uniform across the modeled scenarios. Overall, the selected metrics effectively distinguish the time-varying/precipitation cluster from the fixed-terminus cluster, confirming their suitability for this analysis.

3. Can this methodology be used to distinguish between the endmember climates?

The broad-scale clustering of this analysis is more definitive than distance rankings. This pipeline was able to successfully isolate the fixed terminus cluster. The clustering of the Cold-Icy ADELAM and Warm-Wet Uniform runs to the ground truth can be interpreted in one of two ways. 1) A time-varying terminus does indeed produce morphometry comparable to that created by precipitation. This buttresses the LNIH hypothesis, as it shows that precipitation, whether delivered through rain or snow, is not required to produce the observed branching, dendritic VN. 2) The metrics chosen lack the ability to distinguish between the modeled endmember scenarios. This can be elucidated by improvements in landform evolution modeling techniques, providing more accurate VN for comparison, or by the analysis of a different set of metrics. Since the ensemble of quantitative metrics used has been thoroughly validated by a variety of geomorphic studies, the first interpretation is deemed to be more likely.

References:

[1] Carr, M. H. The martian drainage system and the origin of valley networks and fretted channels. J. Geophys. Res. 100, 7479–7507 (1995) **[2]** Fassett, C.I. and Head III, J.W., 2008. The timing of Martian valley network activity: Constraints from buffered crater counting. Icarus, 195(1), pp.61-89 **[3]** Ramirez, R. et al. Warming early Mars with CO2 and H2. *Nature Geosci* 7, 59–63 (2014) **[4]** Ramirez, R.M., Craddock, R.A. The geological and climatological case for a warmer and wetter early Mars. *Nature Geosci* 11, 230–237 (2018) **[5]** Ramirez, R. et al. Climate simulations of early Mars with estimated precipitation, runoff, and erosion rates. *Journal of Geophysical Research: Planets*, 125, e2019JE006160 (2020) **[6]** F. Forget, R. et al., 3D modelling of the early martian climate under a denser CO_2 atmosphere: Temperatures and CO_2 ice clouds, Icarus 222(1), 81–99 (2013) **[7]** R.D. Wordsworth et al., Global modeling of the early martian climate under a denser CO_2 atmosphere: Water cycle and ice evolution, Icarus 222(1), 1–19 (2013) **[8]** R.D. Wordsworth et al., Comparison of 'warm and wet' and 'cold and icy' scenarios for early Mars in a 3D climate model, Journal of Geophysical Research: Planets 120, 1201–1219 (2015) **[9]** J.L. Fastook & J.W. Head, Glaciation in the Late Noachian Icy Highlands: Ice accumulation, distribution, flow rates, basal melting, and top-down melting rates and patterns, Planetary and Space Science 106, 82–98 (2015) **[10]** Alemanno, G. et al., (2018). Global map of Martian fluvial systems: Age and total eroded volume estimations. Earth and Space Science, 5, 560–577. **[11]** Liu, D. et al. (2024). A global catalog of Martian impact craters with actual boundaries and degradation states. International Journal of Applied Earth Observation and Geoinformation, 131, 103952 **[12]** Howard, A. D. (1994). A detachment-limited model of drainage-basin evolution. Water Resources Research, 30(7), 2261–2285 **[13]** Barnhart, C. J. et al., (2009). Long-term precipitation and late-stage valley network formation: Landform simulations of Parana Basin, Mars. *Journal of Geophysical Research: Planets*, 114(E1), E01003 **[14]** Matsubara, Y. et al., (2013). Hydrology of early Mars: Valley network incision. Journal of Geophysical Research: Planets, 118, 1365–1387 **[15]** Matsubara, Y. et al., (2018). Constraints on the Noachian paleoclimate of the Martian highlands from landscape evolution modeling. *Journal of Geophysical Research: Planets*, 123(11), 2958–2979 **[16]** Laskar, J. et al., (2004). Long term evolution and chaotic diffusion of the insolation quantities of Mars. Icarus, 170(2), 343–364 **[17]** Schorghofer, N. (2008). Temperature response of Mars to Milankovitch cycles. Geophysical Research Letters, 35(18), L18201 **[18]** Palumbo, A.M. & Head, J.W., 2018. Early Mars climate history: Characterizing a "warm and wet" Martian climate with a 3-D global climate model and testing geological predictions. Geophysical Research Letters, 45(19), pp.10-249, **[19]** Palumbo, A.M. et al., 2018. Late Noachian Icy Highlands climate model: Exploring the possibility of transient melting and fluvial/lacustrine activity through peak annual and seasonal temperatures. Icarus, 300, pp.261-286, **[20]** Palumbo, A.M. et al., 2020. Rainfall on Noachian Mars: Nature, timing, and influence on geologic processes and climate history. Icarus, 347, p.113782 **[21]** Scanlon, K. E. et al., (2013). Orographic precipitation in valley network headwaters: Constraints on the ancient Martian atmosphere. *Geophysical Research Letters*, 40(16), 4182–4187 **[22]** Hooshyar, M., Wang, D., Kim, S., Medeiros, S. C., & Hagen, S. C. (2016). Valley and channel network extraction based on local topographic curvature and K-means. *Water Resources Research*, 52, 8081–8102. **[23]** Luo, W., & Stepinski, T. F. (2009). Computer-generated global map of valley networks on Mars. Journal of Geophysical Research: Planets, 114(E11), E11010. **[24]** Luo, W. et al., (2023). Global spatial distribution of Hack's law exponent on Mars consistent with early arid climate. Geophysical Research Letters, 50, e2022GL102604 **[25]** Ansan, V., & Mangold, N. (2013). 3D morphometry of valley networks on Mars from HRSC/MEX DEMs: implications for climatic evolution through time. *Journal of Geophysical Research: Planets*, 118(9), 1873–1894 **[26]** Seybold, H. J. et al., (2018). Branching geometry of valley networks on Mars and Earth and its implications for early Martian climate. *Science Advances*, 4(6), eaar6692 **[27]** Steckel, A. V. et al., (2025). Landscape evolution models of incision on Mars: Implications for the ancient climate. *Journal of Geophysical Research: Planets*, 130(4), e2024JE008637 **[28]** Galofre, A. G. et al., (2020). Valley formation on early Mars by subglacial and fluvial erosion. *Nature Geoscience*, 13(10), 663–668 **[29]** Peckham, S. D. (1995). New results for self-similar trees with applications to river networks. Water Resources Research, 31(4), 1023–1029 **[30]** Rigon, R., Rodriguez-Iturbe et al., (1996). On Hack's law. Water Resources Research, 32(11), 3367–3374

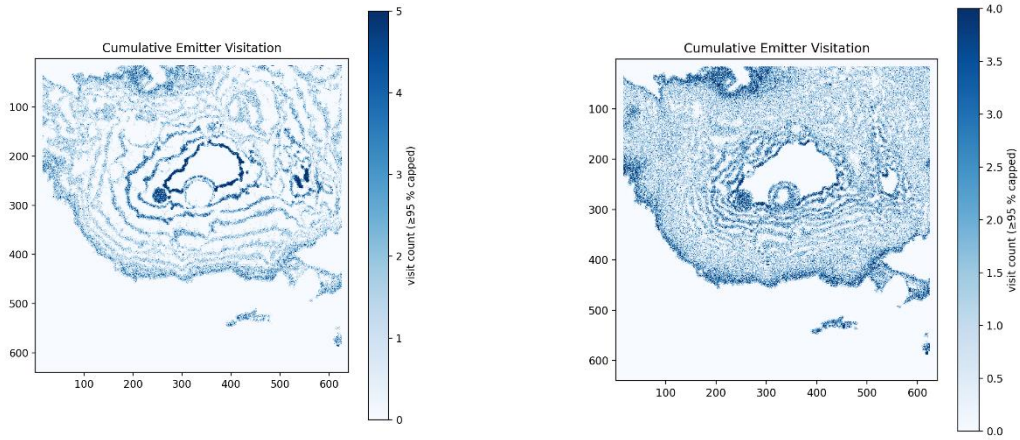

Figure 1. Cumulative visitation of emitter points injected onto the terminus in ADELAM runs. Variable sampling frequency was experimented with in the parameter sweep. Larger gaps can be observed at higher elevations due to the concave up trajectory used in these two runs.

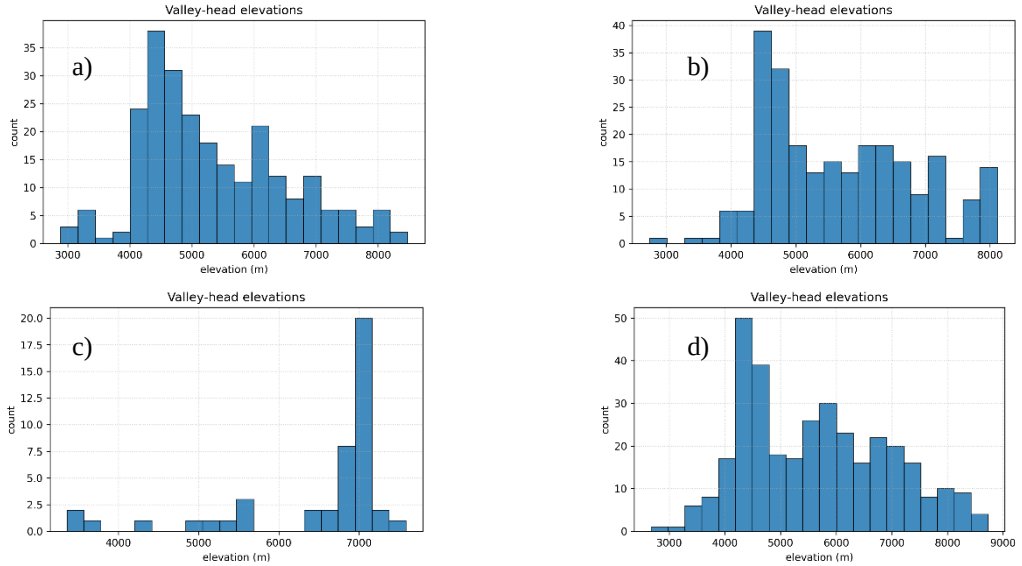

Figure 2. VN headwater elevation distributions for closest match runs. a) Ground Truth. b) ADELAM. c) Cold-Icy Fixed Terminus. d) Warm-Wet Uniform Precipitation. Note the sharp peak exhibited by the Fixed Terminus run, whereas the other three end-member cases display broader, flatter distributions. In particular, ADELAM runs generate valley heads at a wide range of elevations, with a notable concentration at lower elevations.

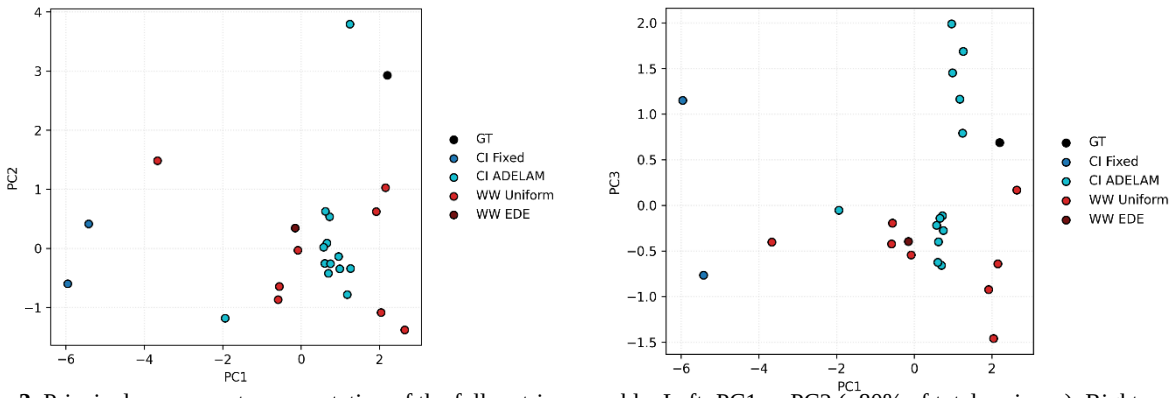

Figure 3. Principal-component representation of the full metric ensemble. Left: PC1 vs PC2 (~80% of total variance). Right: PC1 vs PC3 (~74% of total variance). Ground truth (black) is closest to Cold-Icy ADELAM (cyan). There is overlap between the Warm-Wet Uniform (red) and Cold-Icy ADELAM (cyan) clusters. In both scatter plots, the Cold-Icy Fixed (dark blue) runs can be observed in an isolated cluster on the negative end of PC1 and are ranked last by z-scored Euclidian distance to the ground truth feature.